New Experimental Technique for Determining Real-Space Atomic Images Applied to Aluminum Adsorbed on Silicon (111)

H. Wu and G. J. Lapeyre
Department of Physics, Montana State University, Bozeman, Montana 59717

H. Huang and S. Y. Tong
Laboratory for Surface Studies and Department of Physics, University of Wisconsin-Milwaukee, Milwaukee, Wisconsin 53021
(Received 9 February 1993)

The holographic principle is used to invert experimental photoelectron diffraction spectra to reveal the surface structure of Si(111)($\sqrt{3}\times\sqrt{3}$)-Al. A new transformation method is applied to measured scanned-photon-energy photoemission spectra. The results of each inversion are summed over the set of angles giving images which clearly show the local geometry near the emitting atom, Al. Images are also obtained by theoretical simulation and agree well with experiment. The results demonstrate the technique as a direct, model-independent structural method, yielding bond distances and directions.

PACS numbers: 61.14.−x, 42.40.Ht, 79.60.Dp

Currently there is interest in applying the holographic principle to obtain real-space atomic images of surfaces using measured photoelectron-diffraction spectra [1–5]. The idea is to utilize interference effects of photoelectron waves [6,7]. A photon of energy $h\nu$ is used typically to excite a core-level electron from the element of interest. The final-state outgoing wave from the emitter atom scatters off of neighboring atoms and interferes with the direct outgoing wave from the emitter. It has been pointed out that the interference patterns are similar to a hologram and that a real-space image may be computationally obtained by a Fourier-like transform [6–8]. The intensity of the measured wave is a function of both the photon energy $h\nu$ and the emission direction $\hat{\mathbf{k}}$. Recent experimental image studies, with few exceptions [4,5], focus on the angular dependence in which the photoemission intensity is measured over the emission hemisphere at only one or a few fixed values of $h\nu$, and the image comes from a transform over the angles. This technique is referred to as single-energy holography (SEH). Measurements of SEH can be made at several photoelectron energies and then combined [4,5,9,10]. However, the incident photon energy may be scanned, which changes the de Broglie wavelength k^{-1} of the outgoing electron. In the latter photoemission mode, the initial-state energy is held at a constant value, so the spectroscopy was first termed constant-initial-state energy spectroscopy (CIS) [11,12]. The spectra obtained by the mode have also been referred to as energy-dependent photoelectron diffraction (EDPD) spectra when used with trial and error diffraction calculation to determine interatomic distances [13–16]. This paper uses a new transform for obtaining spatially resolved images by inverting experimental CIS-EDPD spectra in which $h\nu$ is scanned in determining the core-level emission intensity at a number of emission angles [17]. The set of spectra $I_{\hat{\mathbf{k}}}(h\nu)$ is transformed with respect to wave number k to obtain a spatially resolved image. The problems encountered with the SEH approach can be largely eliminated by the scanned photon-energy technique. Here we report an experimental study to test and demonstrate this new technique of obtaining images. The transformed data give good images of the neighboring scattering atoms (Si) with minimal artifacts.

The Si(111)($\sqrt{3}\times\sqrt{3}$)-Al adsorbate structure was selected as a model sample and measured with the radiation continuum available at the Wisconsin Synchrotron Radiation Center (SRC). The "root-three" system has been extensively studied both experimentally and theoretically [18–21]. Measuring the $2p$ emission from the adsorbed Al ensures that backscattering-interference dominates, avoiding the complications resulting from forward focusing and other refraction effects [22]. There are two different threefold hollow sites, T_4 and H_3. It is generally accepted that the Al sits in the T_4 site, with a Si atom directly below it in the second layer. The image from this new data-inversion technique immediately gives this result, which was previously inferred from theory and experiment, but not usually unequivocally determined by experiment [20,21].

The theory describing the photoelectron diffraction and the transform of the spectra into real-space images has been presented earlier [17]. Conceptually, one may view the technique as *vector* extended x-ray absorption atomic fine structure since the transform contains a vector term which gives spatial information, not just a nearest-neighbor distance. The transform for a single CIS spectrum is [17]

$$\phi_{\hat{\mathbf{k}}}(\mathbf{R}) = \int_{k_{\min}}^{k_{\max}} \chi_{\hat{\mathbf{k}}}(k) e^{-ikR} e^{i\mathbf{k}\cdot\mathbf{R}} g(k)\, dk \,, \tag{1}$$

where $\mathbf{R}$ is a vector with its origin at the emitter, Al in this case, and $g(k)$ is a window function for the transform. The normalized CIS spectrum along direction $\hat{\mathbf{k}}$ is given by $\chi_{\hat{\mathbf{k}}}(k) = I_{\hat{\mathbf{k}}}(k)/I_0(k) - 1$, where $I_{\hat{\mathbf{k}}}(k)$ is the measured CIS with the variable changed from $h\nu$ to k (see Fig. 1). The amplitude of the image function is then given by the magnitude of a sum over the set of $\phi_{\hat{\mathbf{k}}}(\mathbf{R})$. The essence of the transformation may be perceived if a

0031-9007/93/71(2)/251(4)$06.00

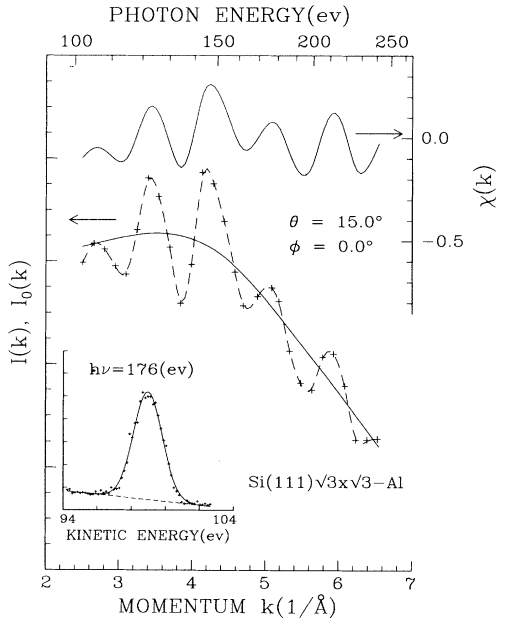

FIG. 1. A representative CIS spectrum $I_{\hat{\mathbf{k}}}(k)$ for Si(111)-$(\sqrt{3}\times\sqrt{3})$-Al with each data point determined from the Al $2p$ EDC shown in the inset. The $I_0(k)$ and $\chi_{\hat{\mathbf{k}}}(k)$ spectra as obtained from $I(k)$.

theoretical expression for $\chi_{\hat{\mathbf{k}}}(k)$ is used and the resulting phase factors are examined [17]. When only single scattering events are considered it is found that the maximum value of the transform is a locus of points given by the solution of $R-\hat{\mathbf{k}}\cdot\mathbf{R}=r_j-\hat{\mathbf{k}}\cdot\mathbf{r}_j$ where $\mathbf{r}_j$ is the position vector of an atom responsible for the scattering. Hence, a CIS measured at a given emission direction $\hat{\mathbf{k}}$ determines a locus of points which defines a surface in real space that is particular to that given direction. Among these points there is one described by $\mathbf{R}=\mathbf{r}_j$ which is $\hat{\mathbf{k}}$ independent; that is, the set of paraboliclike surfaces belonging to a set of CIS's taken in many directions has one point of intersection representing the scatterer located at $\mathbf{r}_j$. In reality these surfaces have a discrete set of crossing points representing all the neighboring atoms. The surfaces are discussed in Ref. [17], multiple scattering events which do not have common crossing points, and hence their contributions to the images are smeared out.

The Si(111)$(\sqrt{3}\times\sqrt{3})$-Al samples were prepared by Al vapor deposition on Si(111)(7×7). The clean-surface valence band and $2p$ core-level spectra have all the known surface features. The experiments were performed on the Iowa State–Montana State beam line with the 2 m grating in the extended-range grasshopper monochromator which scans from threshold to a photon energy of 240 eV. This gives about half of the spectral range considered to be optimal.

By taking advantage of the rotational and mirror plane symmetries of the root-three surface it is sufficient to measure one-sixth of the emission hemisphere of an irreducible symmetry unit. The set of Al $2p$ CIS spectra were taken for a mesh of direction $\hat{\mathbf{k}}$ described by angles (θ,ϕ) in an azimuthal window of $\Delta\phi=60°$ spanning from mirror plane to mirror plane and polar angles from 0° to 60°, which was limited by experimentation technicalities. The polar increments $\delta\theta$ are 7.5°. It took 2 d of beam time to collect the data set of 41 CIS spectra used in this paper, which expands to 193 for the hemisphere. Each point in a CIS spectrum was determined by measuring the energy distribution curve (EDC) for the Al $2p$ core line. For signal normalization, the photon flux was continuously monitored by the photocurrent from a high transmission Ni mesh in the optical path. The area under the line, determined by fitting with a Gaussian and linear background, is used for the CIS intensity $I_{\hat{\mathbf{k}}}(k)$. The photon energy increments are selected to give equal wave-number increments of $\Delta k=0.15$ Å^{-1}. A representative spectrum is shown in Fig. 1. The spectra were collected with a single detector 50 mm spherical electrostatic analyzer collecting about a 2° angular cone (VSW model HA50). The angular settings were obtained with the very precise analyzer goniometer while holding the crystal in a fixed position. The crystal's normal direction is 65° from the impinging-light-beam direction in a configuration which gives optical p polarization where the polarization vector projects onto the sample's mirror plane.

To obtain a function $\chi_{\hat{\mathbf{k}}}(k)$, which is essentially the interference oscillations, for use in the inversion transform requires a determination of $I_0(k)$, a spectral intensity due largely to the differential photoemission cross section. The function is not measurable but can be approximated from the data using one of a number of criteria. In this study the criterion is to find a smooth $I_0(k)$ curve from the $I(k)$ data which passes through the $I(k)$ oscillations as many times as possible and which maximizes the absolute value of the areas formed by the spaces between the I and I_0 curves (see Fig. 1). The smoothness is checked by monitoring the second derivative of I_0. The curves for processing are obtained with a spline fit of the data values [23]. This procedure also takes out the spectral dependent effects due to the throughputs of the photon optical system and the electron optical system as well as small deviations in the light beam–sample–goniometer alignment.

The $\chi_{\hat{\mathbf{k}}}(k)$ functions obtained from the data processing are transformed for various planar cuts on a 0.2 Å grid. Figure 2(a) shows a vertical-plane cut of the image that contains the Al emitter and one first-layer and one second-layer Si atom, where the intensity is shown as the "third" dimension. Note that the origin (0,0) of the image is the Al emitter and hence does not have a feature in the image. The $k_{\min}$ value used is 3.5 Å^{-1} since inclusion of the smaller values degraded the images. The local geometry is sketched in Fig. 2(f). Figure 2(b) shows the image on a horizontal cut passing through the first-layer Si atoms. The shade of each element in the image is a

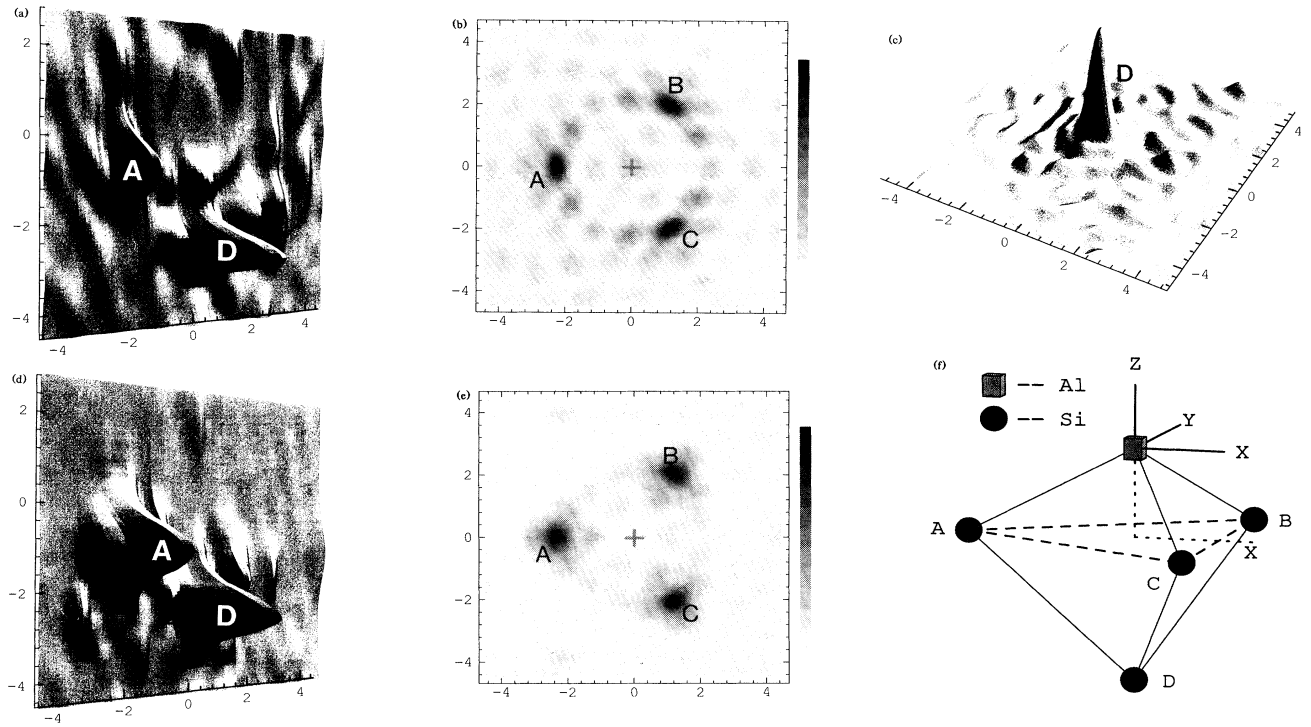

FIG. 2. Image for the surface structure of Si(111)($\sqrt{3}\times\sqrt{3}$)-Al where the Al site is the origin (0,0) and the units are in Å: (a) experimental vertical cut for the plane containing Al (origin), first-layer Si labeled A, and second-layer Si labeled D. (b) Experimental horizontal cut for the plane with the surface Si atoms. (d),(e) Corresponding theoretical simulations, respectively. (c) Experimental horizontal cut for plane with the second-layer Si atom. (f) Sketch of local geometry with letters labeling the Si atoms as labeled on the images.

zero-to-ten grey scale which is proportional to the images' intensity. The horizontal image for the second-layer Si atoms is shown in Fig. 2(c). In Figure 3 are shown three orthogonal line scans for the first- and second-layer Si atoms labeled A and D, respectively. The x-z plane is a mirror plane which is used in the data formatting and forces mirror-plane symmetry in the image.

The experimental results are further examined by comparison with images obtained from similar transformations of EDPD-CIS spectra using multiple scattering calculations which show quite good agreement. The calculations generate spectra in the same angular and energy ranges as the data set by using the structure obtained by dynamical low energy electron diffraction (LEED) analysis [19]. The images obtained from these calculated spectra are shown in Figs. 2(d) and 2(e).

We now comment on the comparisons of images obtained from the theoretical and experimental spectra. For the view in the vertical plane the theoretical image [Fig. 2(d)] agrees well with the experimental image [Fig. 2(a)] where the values for the atomic positions and the FWHM are in close agreement. The second-layer Si atom has a nearly spherical image with some vertical elongation as can be seen in the line scans of Fig. 3. Its positions z_D from experiment, theory, and LEED are -2.6, -2.4, and -2.6 Å, respectively. These values are in very good agreement, particularly since image positions are known to be phase shifted from the correct values due to anisotropic phase shifts $f(\alpha)$ [24]. The good agreement is due to an almost zero (≤ 0.18 Å) slope of the phase of $f(\pi)$ in the Si scattering factor for the energy range used. The radial distance is determined mainly by CIS spectra undergoing a near $-\pi$ scattering at the Si atom. The first-layer nonspherical Si images from theory and experiment also agree very well. The z FWHM is considerably larger but is the same for theory and experiment (1.2 Å), while the x widths differ a bit (0.9 and 0.6 Å, respectively). The horizontal peak positions x_A from experiment, theory, and LEED are -2.3, -2.4, and -2.1 Å, while the depth values z_A are -0.8, -1.1, and -1.2 Å, respectively. Thus the interlayer spacing for Al and the first-layer Si images are phase shifted by amounts not unexpected for this technique. It is, however, interesting to note that the radial distance r_A from Al to the first layer Si is 2.45, 2.65, and 2.5 Å, respectively, showing variations which are quite similar to those radial-distance values for the second-layer Si atoms. This is again due to the small slope of $f(\pi)$. The good agreement between image position and the correct radial distance is probably fortuitous and generally should not be expected to hold. The agreement in the present case is largely a result of the rather weak Si

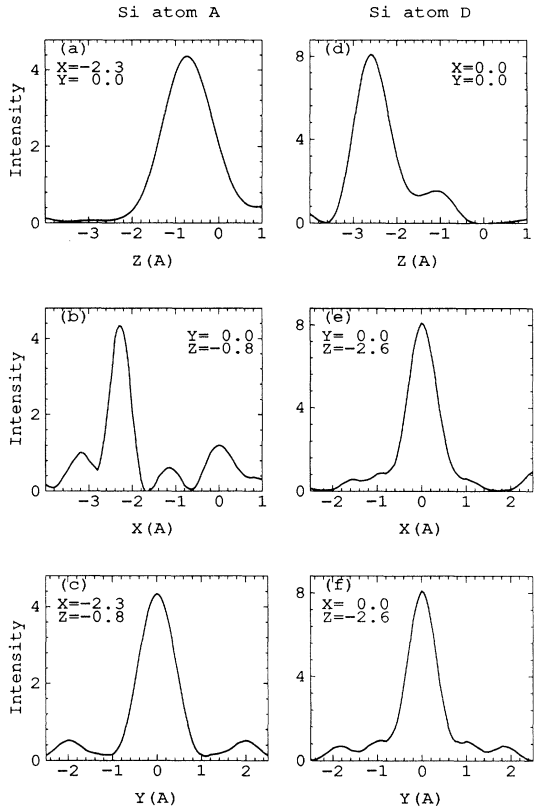

FIG. 3. Experimental line scans of the image intensities for Si in the Si(111) $(\sqrt{3}\times\sqrt{3})$-Al structure. Three orthogonal directions for the first-layer Si in panels (a), (b), and (c) (labeled *A*) and for the second-layer Si in panels (d), (e), and (f) (labeled *D*). Al is the origin of the image and the units are in Å.

scattering and the relatively low kinetic energies used in the measurement (50 to 200 eV).

This work demonstrates that images with atomic resolution can be obtained by using photoemission spectra obtained in the CIS mode. The technique promises significant contributions to sorting out the properties of adsorbate systems by directly determining site position. Such direct information should simplify the utilization of trial and error diffraction techniques.

A previously proposed inversion approach is to scalar transform CIS spectra in a method known as angular-resolved photoemission fine structure (ARPEFS) [25]. The structural information obtained by ARPEFS is scattering path-length differences between an emitting atom and its neighbors. ARPEFS is not a direct method because surface models are still needed to simulate probable path-length differences. A more severe difficulty of ARPEFS is that multiple and single scattering path-length differences are indistinguishable. The method does not produce the three-dimensional structural information obtained with CIS holography in this work. In the method demonstrated here, distances and orientations of surface atoms relative to the location of an emitter site are simultaneously obtained from inversion of measured spectra with no model calculation necessary. Multiple scattering artifacts are eliminated through adding the complex amplitudes $\phi_{\hat{\mathbf{k}}}(\mathbf{R})$ in Eq. (1) over a set of $\hat{\mathbf{k}}$ directions [17].

We acknowledge contributions to the laboratory work by Montana State University (MSU) students Hong Yu and Zhu Lin. The help and support of Jim Anderson, Cliff Olson, and the SRC staff are greatly appreciated. Grants from NSF support the MSU effort (No. DMR-9107854) and the SRC facility (No. DMR-9212658). NSF provided an instrumentation grant for the construction of the Iowa State University and Montana State University beam line. Work by S.Y.T. is supported by ONR, Grant No. 000-14-90-J1749.

[1] G. K. Harp, D. K. Saldin, and B. P. Tonner, Phys. Rev. Lett. **65**, 1012 (1990).
[2] S. A. Chambers, V. A. Loebs, Hua Li, and S. Y. Tong, J. Vac. Sci. Technol. B **10**, 2092 (1992).
[3] G. S. Herman, S. Thevuthasan, T. T. Tran, Y. J. Kim, and C. S. Fadley, Phys. Rev. Lett. **68**, 650 (1992).
[4] L. J. Terminello, J. J. Barton, and D. A. Lapiano-Smith, J. Vac. Sci. Technol. B **10**, 2088 (1992).
[5] H. Li *et al.*, Phys. Rev. B **47**, 10036 (1993).
[6] A. Szoke, in *Short Wavelength Coherent Radiation Generation and Applications*, edited by D. T. Attwood and J. Boker, AIP Conf. Proc. No. 142 (AIP, New York, 1986).
[7] J. J. Barton, Phys. Rev. Lett. **61**, 1356 (1988).
[8] S. A. Chambers, Surf. Sci. Rep. **16**, 261 (1992).
[9] J. J. Barton, Phys. Rev. Lett. **67**, 3102 (1991).
[10] S. Y. Tong *et al.*, Phys. Rev. Lett. **67**, 3102 (1991).
[11] G. J. Lapeyre *et al.*, Solid State Commun. **15**, 1601 (1974).
[12] G. J. Lapeyre *et al.*, J. Phys. (Paris), Colloq. **39**, C4-134 (1978).
[13] S. Y. Tong and C. H. Li, Bull. Am. Phys. Soc. **23**, 417 (1978); C. H. Li and S. Y. Tong, Phys. Rev. B **19**, 1769 (1979).
[14] S. D. Kevan *et al.*, Phys. Rev. Lett. **41**, 1565 (1978).
[15] S. D. Kevan *et al.*, Phys. Rev. Lett. **46**, 1629 (1981).
[16] R. Dippel, D. P. Woodruff, X.-Mu. Hu, M. C. Asensio, A. Robinson, K. M. Schindler, K. U. Weiss, P. Gardner, and A. M. Bradshaw, Phys. Rev. Lett. **68**, 1543 (1992).
[17] S. Y. Tong *et al.*, Phys. Rev. B **46**, 2452 (1992).
[18] J. E. Northrup, Phys. Rev. Lett. **53**, 683 (1984).
[19] H. Huang *et al.*, Phys. Rev. B **42**, 7483 (1990).
[20] R. J. Hamers and J. E. Demuth, J. Vac. Sci. Technol. A **6**, 512 (1988).
[21] R. I. G. Uhrberg *et al.*, Phys. Rev. B **31**, 3805 (1985); J. M. Nicholls *et al.*, Phys. Rev. B **35**, 4137 (1987).
[22] A. Stuck *et al.*, Surf. Sci. **264**, 380 (1992).
[23] Used software in GENPLOT from Computer Graphic Service, 52 Genung Circle, Ithaca, NY 14850.
[24] S. Y. Tong *et al.*, Phys. Rev. Lett. **66**, 60 (1991).
[25] Z. Hussain *et al.*, Proc. Natl. Acad. Sci. U.S.A. **78**, 5293 (1981); J. J. Barton *et al.*, Phys. Rev. Lett. **51**, 272 (1983).

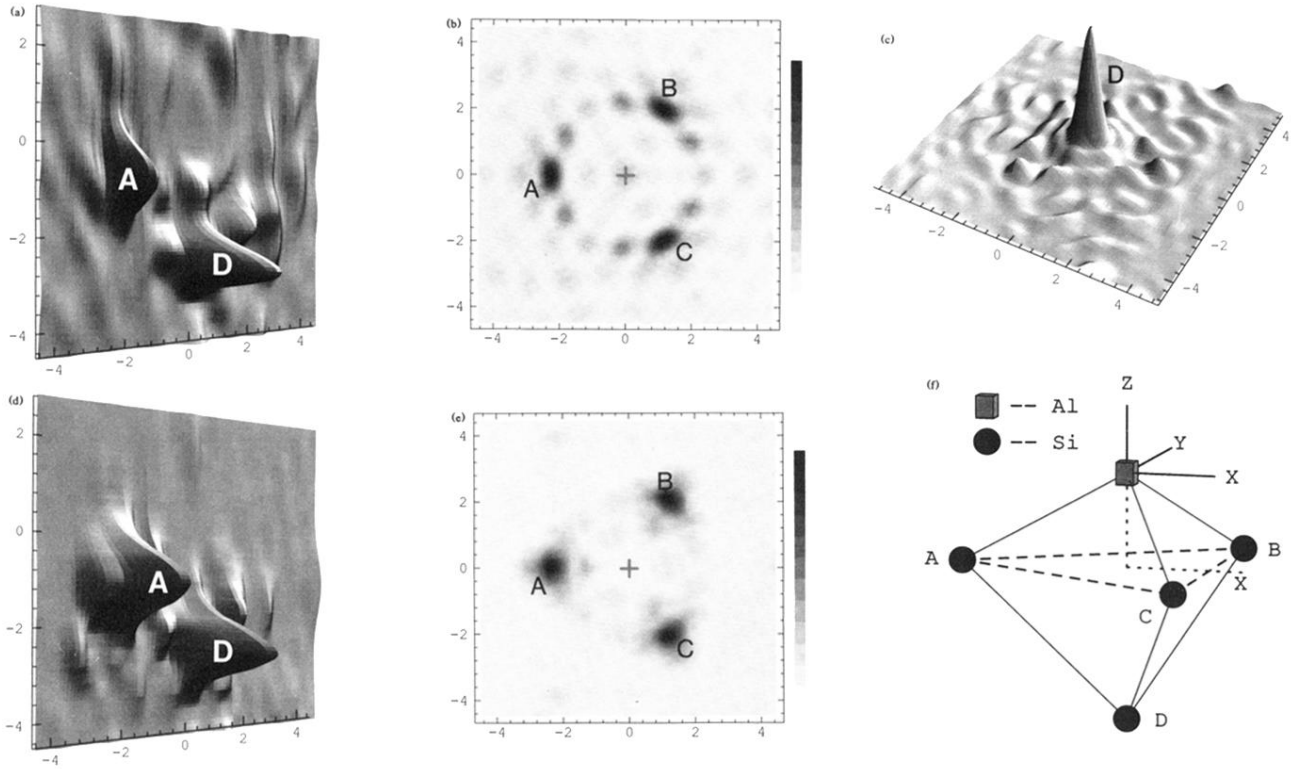

FIG. 2. Image for the surface structure of Si(111)($\sqrt{3}\times\sqrt{3}$)-Al where the Al site is the origin (0,0) and the units are in Å: (a) experimental vertical cut for the plane containing Al (origin), first-layer Si labeled *A*, and second-layer Si labeled *D*. (b) Experimental horizontal cut for the plane with the surface Si atoms. (d),(e) Corresponding theoretical simulations, respectively. (c) Experimental horizontal cut for plane with the second-layer Si atom. (f) Sketch of local geometry with letters labeling the Si atoms as labeled on the images.